https://doi.org/10.21289/KSIC.2022.25.6.953

Development of Robotic Tools for Chemical Coupler Assembly

Sung-Hun Jeong[1], Gi-Seong Kim[2], Shi-Baek Park[3], Han-Sung Kim[4*]

〈Abstract〉

In this paper, the design result of robotic tools and the development of robot control system for chemical coupler assembly are presented. This research aims to eliminate the risk of chemicals exposed to human operators by developing the robotic tools and robot automation system for chemical tank lorry unloading that were done manually. Due to tight tolerance between couplers, even small pose error may result in very large internal force. In order to resolve the problem, the 6-axis compliance device is employed, which can provide not only enough compliance between couplers but also F/T sensing. The 6-axis compliance device having large force and moment capacity is designed. A simple linear gripper with rack-and-pinion is designed to grasp two sizes of couplers. The proposed robot automation system consists of 6-DOF collaborative robot with offset wrist, 6-axis compliance device with F/T sensing, linear gripper, and two robot visions.

Keywords : Chemical Coupler Assembly, Position/Force Control, Collaborative Robot with Offset Wrist, 6-axis Compliance Device, Linear Gripper

1 Dept. of Mechanical Convergence Engineering, Kyungnam University
E-mail: rpdmdrpdm@naver.com
2 Dept. of Mechanical Convergence Engineering, Kyungnam University
E-mail: shark-cat@daum.net
3 Samsung Electronics, GCS Team, Staff Engineer
E-mail: shibaek.park@samsung.com
4* Corresponding author, Dept. of Mechanical Engineering, Kyungnam University, Professor
E-mail: hkim@kyungnam.ac.kr

1. Introduction

In the semiconductor industry, more than 100 kinds of chemicals are supplied through the central chemical supply system (CCSS) for the purposes of cleaning, etchant, stripper, electroplating, etc. In semiconductor processes such as cleaning, photo, chemical vapor deposition (CVD), metal interconnect, and so on, the filling method using tank lorry and drum is used to input chemicals to these CCSS. Among them, the filling through the tank lorry is fastened with a coupler for filling by a worker equipped with chemical protective equipment. This work is highly dangerous because it can be directly exposed to chemicals and their fumes [1].

With the development of modern automation development technology, many tasks that could only be done by human operator have been started to be automated [2-3]. In particular, automation of hazardous tasks is attracting great attention in industries that use chemical substances or nuclear power that are directly hazardous to humans [4-6].

Handling chemical coupler between tank lorry and ACQC (Automatic Clean Quick Coupler) system may be hazardous or toxic to human operators, therefore robot automation is essential. This research aims to eliminate the risk by developing a collaborative robot for chemical tank lorry unloading that were done manually. Due to tight tolerance between couplers, small pose error may result in very large internal force. In order to resolve the problem, compliance between the robot end-effector and the male coupler should be introduced with 6-axis compliance device with F/T(Force/Torque) sensing.

In this paper, the design result of robotic tools and the development of robot control system for chemical coupler assembly are presented. A simple design method of a 6-axis compliance device having decoupled stiffness is presented. The 6-axis compliance device prototype is designed with six simple beams and strain gauges, which is used to control the position/force at the same time [7]. The linear gripper with actuator module and rack-and-pinion mechanism is designed and controlled to grasp two sizes of couplers. Finally, the development of the robot system is presented, which consists of a 6-DOF collaborative robot, a 6-axis compliance device, a 1-axis linear gripper, and two robot visions.

2. Compliance Device Design

The position/force control is to control displacement and force at the same time between the tool of a robot and workpiece by using a compliance device mounted on the end-effector of a robot. In previous research, the compliance device with 6-$S\underline{P}S$ mechanism [8] was developed, which S and P denote spherical and prismatic joints, respectively. The underbar of $\underline{P}$ indicates that spring or compliant element is installed at the P joint. The previous prototype consists

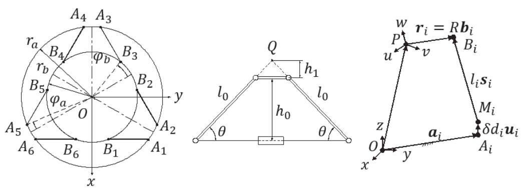

(a) Top view (b) Front view (c) Vector-loop

Fig. 1 Geometry of a 6-$\underline{P}SS$ compliance device

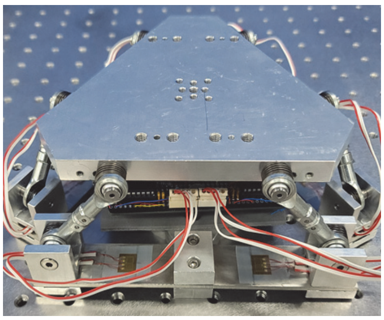

Fig. 2 6-$\underline{P}SS$ compliance device prototype

of linear springs and linear optical encoders in the cylinders and provides high force resolutions. However, the size is relatively large, and the optical sensor is susceptible to dust and oil. In order to overcome the disadvantages, the compliance device of 6-$\underline{P}SS$ mechanism with cantilever beams and strain gauges (Fig. 2) is presented, which can be fabricated with smaller size and is not sensitive to chemicals.

From the kinematics relations (Fig. 1), the Jacobian matrix [9] is given by

$$J_x^T \delta \boldsymbol{D} = J_q \, \delta \boldsymbol{q} \text{ or } \delta \boldsymbol{q} = (J_x \, J_q^{-1})^T \delta \boldsymbol{D} = J^T \delta \boldsymbol{D} \quad (1)$$

where the Jacobian submatrices are

$$J_x = \begin{bmatrix} \boldsymbol{s}_1 & \cdots & \boldsymbol{s}_6 \\ \boldsymbol{r}_1 \times \boldsymbol{s}_1 & \cdots & \boldsymbol{r}_6 \times \boldsymbol{s}_6 \end{bmatrix}, J_q = diag(\boldsymbol{s}_1^T \boldsymbol{u}_1, \cdots, \boldsymbol{s}_6^T \boldsymbol{u}_6) \quad (2)$$

The statics relations can be obtained using the principle of virtual work by

$$\boldsymbol{w} = (J_x \, J_q^{-1}) \boldsymbol{\tau} = J \boldsymbol{\tau} \quad (3)$$

Using the beam stiffness ($\tau_i = k_i \, \delta d_i$), the stiffness mapping of the compliance device is given by

$$\boldsymbol{w} = [J_x (J_q^{-1} [k] J_q^{-T}) J_x^T] \delta \boldsymbol{D} = K \delta \boldsymbol{D} \quad (4)$$

The Cartesian stiffness matrix at the center of compliance, Q is given by

$$K = k \times diag(3\cot^2\theta, 3\cot^2\theta, 6\,; \; 3r_b^2\cos^2\phi_b, 3r_b^2\cos^2\phi_b, 6r_b^2\cos^2\phi_b\cot^2\theta) \quad (5)$$

where $k \equiv k_1 = \cdots = k_6$. Among the design parameters, the inclined angle of a leg ($\theta = 49.46^\circ$) plays an important role in balancing the stiffness ratio between the stiffnesses along and about the xy and z axes. For cantilever beam parameters (width ($b = 25$mm), thickness ($h = 3.3$mm), length ($l = 60$mm), $E = 193$GPa (SUS304)), the beam stiffness is calculated by

$$k = \frac{3EI}{l^3} = \frac{Ebh^3}{4l^3} = 200.68 \; [N/mm]$$

The Cartesian stiffness matrix at the center of compliance ($h_1 = 43.84$mm) is determined by

$$K = diag(440, 440, 1204 [N/mm]; \; 2277, 2277, 3332 [Nm/rad])$$

The maximum load capacities and the

Table 1. Specifications of the 6-axis compliance device

Axes	f_x	f_y	f_z	n_x	n_y	n_z
Max. load [N][Nm]	415	360	840	30	26	44.5
Max. deflection [mm][deg]	0.54	0.47	0.4	0.44	0.38	0.44
Dimensoins (H×W×L)	183×211×71		Weight[kg]	1.38		

Table 2. Joint and Cartesian calibration results

Joint axes	1-axis	2-axis	3-axis	4-axis	5-axis	6-axis
Gain [mV/N]	13.924	13.881	14.334	14.223	14.660	15.195
Cartesian axes	f_x	f_y	f_z	n_x	n_y	n_z
RMSE [N][Nm]	0.173	0.448	0.402	0.032	0.023	0.067

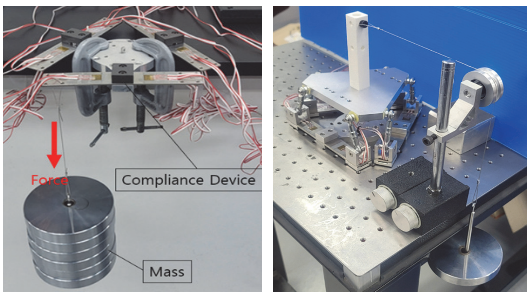

Fig. 3 Joint and cartesian calibration experiments

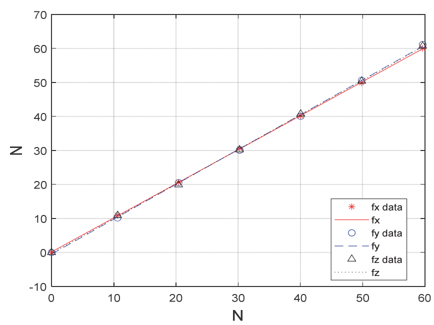

(a) Force measurement

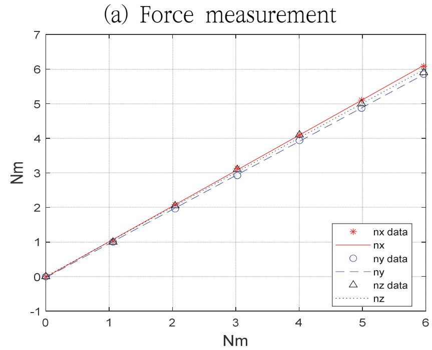

(b) Moment measurement

Fig. 4 Verification of force and moment measurements

maximum deflections at Q along and about the x-, y-, and z-axis are given in Table 1.

Differently from commercial F/T sensors with cross beam structure, the force and moment of the proposed compliance device can analytically be calculated by Eq. (3), once joint forces are measured by strain gauge on simple beam. The joint calibration on strain gauge measurements are performed and the calculated force and moment using the statics equation are compared with applied force and moment as shown in Fig. 3. Fig. 4 shows the linearities of applied force/moment (x-axis) and calculated force/moment (y-axis). Finally, the calibrated joint gains and the resulting RMSE (RMS error) are given in Table 2.

3. Linear Gripper Design

As shown in Fig. 5, three gripper mechanisms grasping chemical couplers may be considered. First one can be fabricated with small volume, however kinematics calculation is required and gripping force is relatively small [10-13]. Second one can provides large gripping force, however gripper base becomes very large due to ball screw assembly [14]. In this work, rack-and-pinion mechanism is selected because it is more compact than ball screw type and provide relatively large grip force.

Fig. 6 shows the linear gripper design in detail, which consists of an actuator module with hollow BLDC motor and harmonic drive, rack-and-pinion mechanism with linear guide, and finger tips grasping both 20A (outer diameter, D=27.2mm) and 50A (D=60.5mm) couplers. The linear gripper prototype is fabricated in Fig. 7, and the specifications of the linear gripper are given in Table 3.

The gripper controller uses an EtherCAT servo drive and the CST (Cyclic Synchronous Torque) mode. Simple PD control method is employed in moving fingers and in grasping an object, a specified torque is held. Fig. 8 shows the gripper control experiments for

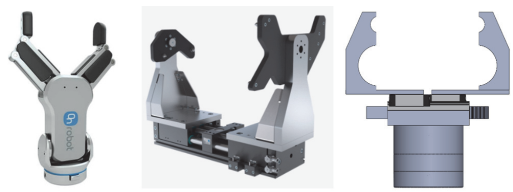

(a) (b) (c)

Fig. 5 Comparison of linear gripper designs for (a) linkage gripper (Onrobot), (b) ball screw gripper (Zimmer) and (c) rack-and-pinion gripper

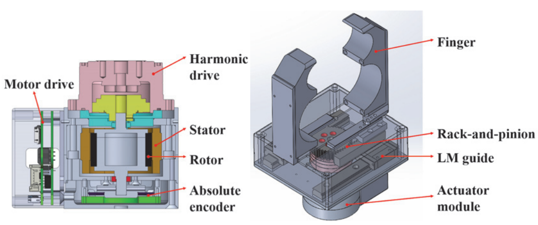

(a) Actuator module (b) Linear gripper

Fig. 6 Linear gripper design

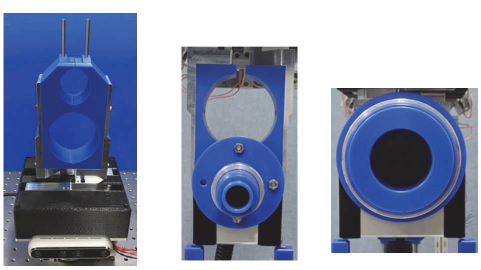

(a) Prototype (b) 20A coupler (c) 50A coupler

Fig. 7 Gripper prototype and coupler grasping with linear gripper

Table 3. Specifications of the actuator and gripper (Allied Motion MF0060020 + Harmonic drive CSF-17-50-2UH + GEAHS1.5-40-15-A-10)

Motor output		Gear output	
Torque[Nm]	0.54	Torque[Nm]	27.0
Speed[rps]	56.37	Speed[rps]	1.12
Grip force[N]	450	Grip stroke[mm]	106

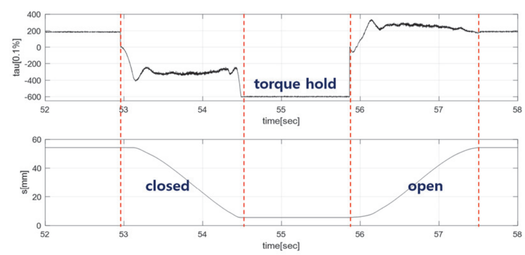

(a) 20A coupler

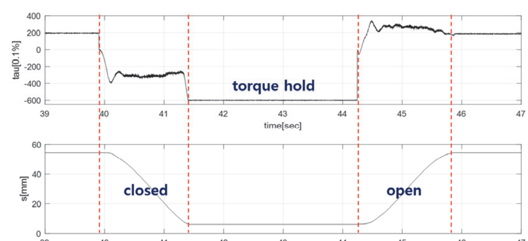

(b) 50A coupler

Fig. 8 Linear gripper control results according to coupler grasping

20A and 50A coupler. It is shown that in closed and open modes, torque is varying according to PD control law, however in grasping mode, torque is held in constant with the specified 60% of nominal motor torque.

4. Robot Automation System

The robot automation system assembling chemical coupler between tank lorry and ACQC system has been developed in Fig. 9. The robot automation system is made up of a 6-DOF collaborative robot which will be mounted on a mobile platform, 6-axis compliance device with F/T sensing, linear gripper, and two robot visions.

Specifically, a 6-DOF collaborative robot with 16kg payload was developed considering heavy robotic tools and the weights of 50A male coupler and hose containing chemicals. The collaborative robot with offset wrist is selected due to narrow working environment in ACQC system and its collision detection function. The proposed robot manipulator with offset wrist has the advantage of higher payload and less singularity than other collaborative counterparts. The specifications of the developed collaborative robot are given in Table 4 [15].

As shown in Fig. 10, the control system consists of a host PC for teaching pendant, two target PCs for the real-time control of the robot with six EtherCAT drives and the gripper with one EtherCAT drive, and six strain gauge amplifiers.

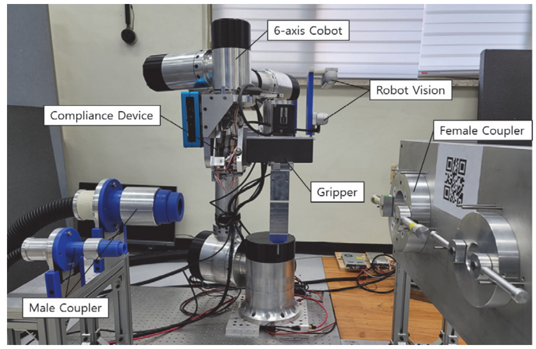

Fig. 9 Robot automation system development for chemical assembly

Table 4. Specifications of a 6-axis collaborative robot

Specifications	Value
No. of axes	6
Payload	16kg
Reach	1,300mm
Repeatability	0.11mm

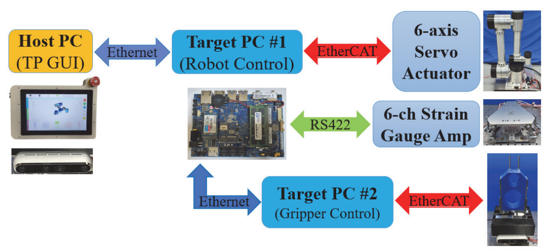

Fig. 10 Control system configuration

Acknowledgement

This research was partially supported by Samsung Electronics-University Cooperation Research Project.

References

[1] S-B. Park, et al., “Development of Chemical Drum Auto-connection Module,” Proc. Kor. Soc. Prec. Eng. pp. 238-238, (2020).
[2] S. Micheler, et al., “A Transformation of Human Operation Approach to Inform System Design for Automation,” J. Int. Manu. vol. 32, pp. 201-220, (2021).
[3] R. Verbiest, et al., “Automation and Robotics in the Cultivation of Pome Fruit: Where do we stand today?,” J. Field Robotics. pp. 1-19, (2020).
[4] J. Y. Pan, “Engineering Chemistry Innovation,” ACS Med. Chem. Lett. vol. 10, pp. 703-707, (2019).
[5] M. Starý, et al., “Sampling Robot for Primary Circuit Pipelines of Decommissioned Nuclear Facilities,” Auto. Cons. vol. 119, 103303, (2020).
[6] C. Ducros, et al., “RICA: A Tracked Robot for Sampling and Radiological Characterization in the Nuclear Field,” J. Field Robotics. vol. 34, pp. 583-599, (2017).
[7] M. Griffis, and J. Duffy, “Kinestatic Control: A Novel Theory for Simultaneously Regulating Force and Displacement,” Trans. ASME Journal of Mechanical Design. vol. 113, no. 4, pp. 508-515, (1991).
[8] H. S. Kim, “Kinestatic Control using Six-axis Parallel-type Compliant Device,” KSMTE, vol. 23, pp. 421-427, (2014).
[9] H. S. Kim, “Design of a 6-axis Compliance Device with F/T Sensing for Position/Force Control,” Journal of the Korean Society of Industry Convergence, vol. 21, no. 2, pp. 63-70, (2018).
[10] G. S. Kim, and H. S. Kim, “Study on the Design of a Novel Adaptive Gripper,” Journal of the Korean Society of Industry Convergence, Vol. 22, No. 3, pp. 325-335, (2019).
[11] S. Montambault, and C. M. Gosselin, “Analysis of Underactuated Mechanical Grippers,” Transactions of the ASME, Vol. 123, pp. 367-374, (2001).
[12] https://robotiq.com
[13] https://onrobot.com/ko
[14] https://www.zimmer-group.com/ko
[15] G. S. Kim, and H. S. Kim, “Inverse Kinematic Analysis of a 6-DOF Collaborative Robot with Offset Wrist,” Journal of the Korean Society of Industry Convergence, vol. 24, no. 6, pp. 963-959, (2021).

Manuscript received November 08, 2022;
revised November 30, 2022; accepted December 05, 2022